I.J. Image, Graphics and Signal Processing, **2023, 1, 23-35**
Published Online on February 8, 2023 by MECS Press (http://www.mecs-press.org/)
DOI: 10.5815/ijigsp.2023.01.03

Detecting the Third Heart Sound: Separation and Localization from Lung Sound using Intrinsic Time Scale Decomposition

Sai Bharadwaj B*
Department of Electronics & Communication Engineering, Vignan's Institute of Engineering for Women, Visakhapatnam, Andhrapradesh, India, PIN 530049
Email: research4816@gmail.com
ORCID: https://orcid.org/0000-0002-2476-3825
*Corresponding author

Ch. Sumanth Kumar
Dr.Ch. Sumanth Kumar, Department of Electrical, Electronics and Communications, GITAM Institute of Technology, GITAM Deemed to be University, Visakhapatnam, Andhrapradesh, India

Received: 02 June, 2022; Revised: 16 July, 2022; Accepted: 19 September, 2022; Published: 08 February, 2023

Abstract: The extraction of heart sound component from a composite signal of heart and lung is a quite challenging task in phonocardiogram signal analysis the first heart sound (S1) and the second heart sound (S2), produced by the closing of the atrioventricular valves and the closing of the semilunar valves, respectively, are the fundamental sounds of the heart. To accomplish this task a novel framework with intrinsic time scale decomposition (ITD) is designed. The capture of the PCG signal frequently hides the detection of the third heart sound (S3), which is necessary to identify cardiac failures. To separate S3, ITD method is deployed to enable signal decomposition into certain levels. Next, by applying smoothed pseudo-Wigner Ville distribution (SWVD) with reassignment, the location of S3 is detected. The proposed method is performed on 36 combinations consists of 144 cardiac cycles containing S3 obtained from different online databases. In comparison to existing approaches, the proposed work separates the S3 from other heart and lung sounds and the proposed method obtained the detection accuracy of S3 as 95.4%, which proves the superiority with other methods.

Index Terms: Phonocardiogram signal, intrinsic time scale decomposition, smoothed pseudo-Wigner Ville distribution, localization of heart sound.

1. Introduction

Generally, when a patient visits a medical facility (a clinic, doctor's office, hospital, etc.) to assess his cardiovascular health, the doctor first performs auscultation, typically through a stethoscope, to listen to lung and heart sounds, looking for abnormalities and making a preliminary diagnosis based on his experience and hearing skills [1]. The doctor can next request an electrocardiogram (ECG) or an echocardiogram, both of which are pricey exploratory tools that call for trained and experienced individuals to do the tests and analyze the results, if a cardiac issue is detected [2]. Therefore, the creation of simple, affordable, accurate, and dependable exploration and diagnostic tools, like those found on smartphones, is crucial for today's society, which is eager to take charge of its own health patient empowerment The PCG signal comprises bioacoustics data that can be used to diagnose cardiovascular disease and evaluate cardiac function. This data tells how the heart is working and in what condition it is [3]. The mechanical events of the heart are controlled by the myocardium's depolarization and repolarization in response to the sinoatrial node triggering, which is illustrated by the electrical signal in the ECG and the acoustic signal illustrated by a PCG. While the ECG provides information about the electrical activity of the heart, the PCG provides information about the noises made by the mechanical activity (acoustic vibrations) of the heart [4] Significant research in electronic sensing of heart sounds and diagnosis of heart diseases is greatly improved. El-Segaier et.al [5] described the procedure for sensor-based detection system in heart sound signal analysis. The electronic system analysis can quantify variations in heart sounds through different signal processing stages [6]. The heart sounds are recorded by placing the digital stethoscope at fourth

intercoastal area. This sound signal which is acquired from left side of the chest contains dominant heart sounds than lung sounds [7]. However, when heart sounds are considered and recorded from the chest area, lung sounds are mixed and collected up. This unavoidable interference of lung sounds can be separable from heart sounds using digital signal processing methods. The lung sounds are observed due to flow of air with in the lungs during respiration process. Abnormal breath sounds occur when the air is obstructed by pulmonary deficiency. The low and high pitch normal breath sound frequency ranges from 100-1KHz and 100-5KHz, for high pitch observed a spectral overlap with heart sounds. Heart sounds are generated due to physical opening and shutting of heart valves. The first heart sound S1's frequency range is from 10-120Hz, the second heart sound, S2's frequency range is from 120-200Hz, The S1 and S2 are considered as normal sounds. The abnormal heart sounds incorporate the third and fourth heart sound constituted by S3 & S4 respectively. The frequency range is 20-40Hz for S3 and 40-80Hz for S4 [8].

Several studies made to use different methods in separating the Heart and Lung (HL) sound signals. Some of them are based on adaptive filtering [9,10] this requires prior information of the signal. Wavelet based filtering introduced in [11] reported that heart sounds were not separated fully from lung sounds. Pourazad et.al [12] used time frequency filtering which was separated the heart sounds successfully. Empirical mode decomposition (EMD) has reported in [13], is an advanced technique for nonlinear signal analysis. Entropy based methods were introduced by Yadollahi [14] localized heart sounds, proved that the results are better with Shannon entropy than Renyi entropy. Single spectrum analysis [15], was confirmed as a significant method in detaching the heart sound components. The main objectives of heart sound detection methods are to pinpoint S3 in the presence of lung noises. For pregnant women, youngsters, and participants in intense activities, S3 displays a typical indication, but it is a serious one for those over 40 [16]. The observed S3 in the diastolic period, which occurs 100–150 ms following the S2, is a crucial clinical marker for the diagnosis of heart failure [17]. Transform techniques like short time Fourier transform, S Transform, and wavelet transform were used in many studies The majority of earlier research in the S3 detection were based on time frequency representation (TFR). A comparative analysis was made by Sejdic and Jiang [18] on these three techniques and noticed an uplifted result for S-Tranform. Kumar et.al [19] used wavelet transform to recognize S3 from the background noise. In a recent study on time frequency representation algorithms, re assigned smoothed pseudo-Wigner Ville distribution [20] was proved the capability of localizing the overlapped time components. A powerful nonlinear decomposition technique, Hilbert vibration decomposition (HVD) was used in combination with re assigned smoothed pseudo-Wigner Ville distribution (RSWVD) for the detection of S3 component [21]. Although it requires experience to detect precise auscultation of the third heart sound because this condition is associated with cardiovascular mortality. Hence ITD was introduced to detect the heart and lung sound without any time delay. Hence the major contribution of the paper is as follows:

- To enhance the detection capability, S3 is separated using ITD and RSWVD techniques in which signal decomposition into certain levels is enabled and hence S3 location is detected by using pseudo-Wigner Ville distribution (SWVD) with reassignment method.
- To show the effectiveness of ITD and RSWVD techniques, quantitative comparisons are made with EMD and HVD technique with parameters like mean square error, signal to error ratio and the correlation factor.

The paper organizes as follows. Section 2 propounds briefly about the proposed system. Section 3 introduces about the methods. Experiment methodology is described in section 4. Section 5 displays results and discussions followed by conclusions in section 6.

2. Literature Survey

Zeng et al [22] suggested a system that classifies anomalies (normal vs. abnormal) automatically from PCG data without segmenting the heart sound signals. To model, identify, and detect abnormal patterns in the dynamics of the PCG system caused by heart disease, representative features are extracted using hybrid signal processing and artificial intelligence tools, such as the tunable Q-factor wavelet transform (TQWT), variational mode decomposition (VMD), phase space reconstruction (PSR), and neural networks. The TQWT method is used to break down the heart sound signal into a number of frequency sub bands with various levels of decomposition. Then, VMD is used to separate the heart sound signal's sub band into various intrinsic modes. The first four intrinsic modes are thought to be the primary intrinsic modes because they contain the majority of the signal's energy. They are chosen to build the analysis's reference variable. Thirdly, the reference variable's phase space is rebuilt while maintaining the characteristics of the nonlinear PCG system dynamics. However, it does not have mathematical relationship between the embedding dimension, time lag, Q-factor, redundancy, decomposition level and the classification accuracy and also it does not regroup the database in a patient wise manner.

Altuve et al [23] provided valuable information about the functioning and state of the heart that is useful in the diagnosis of cardiovascular diseases. The fundamental sounds of the heart are the first heart sound (S1) and the second heart sound (S2), which are created by the atrioventricular and semilunar valves closing, respectively. It is challenging to use these heart sounds in computer systems to produce an automatic diagnosis due to the closeness in shape and length of these heart sounds as well as their superposition in the frequency domain. Additionally, by analyzing the

time-frequency representation of PCG recordings, it may be possible to automatically identify heartbeats and identify diseases based on their distinctive patterns in the IMF. The variance and Shannon's entropy of the heart sounds, which were recorded in time frames scattered across several IMF, were analyzed. Hence also used both methods to decompose the PCG recordings in order to identify the frequency ranges of the IMF. These heart sounds were represented in different IMF with different variances and entropies in both techniques because the frequency content of S1 and S2 differs but overlaps, and the duration of these sounds is also different. However, the visual inspection of these IMF does not clearly represent the heart sounds.

Nishi et al [24] analyzed the problem of expensive and ineffective diagnostic techniques currently in use can be solved by using respiratory sound to diagnose lung disorders in a cost-effective, non-invasive, accurate, and affordable manner. During the breathing process, the air flow pressures the walls of the respiratory organs, producing sounds that may be heard by placing a stethoscope over the chest walls. These sounds are known as respiratory sounds or lung sounds. During the capture of the respiratory sound, a variety of noises can overlap with it, including recording artefacts, heart sound interferences, power line interferences, and ambient acoustic interferences. The vibration of blood flowing against the cardiac valve as it opens and closes during the cardiac cycle causes heart sounds to be created. Noise can be thought of as the unwanted and unavoidable non-breathing signal that interferes with the quality of the genuine respiratory sound signal. If the respiratory sound stream is noise-free, computerized interpretations based on it will become more and more successful. However, it does not suppress the HS contaminations from lung sound signals and also not tested on lung sounds recorded at the different air flow rate.

Sangeetha et al [25] suggested Lung sound signals can be denoised using an adaptive threshold Empirical Mode Decomposition (aEMD) technique, which enhances the signal's quality and makes it easier to detect respiratory diseases. The most crucial technique for identifying lung problems is auscultation and acoustic examination of lung sounds. Lung noises are mostly caused by the fast changes in gas pressure or the oscillations of solid tissues. During auscultation, heart sound (HS), background noise, thoracic tissue effects, and measurement noise contaminate the lung sounds that are captured. Modern stethoscopes can assist in hearing the sounds more clearly, but heart sounds continue to interfere with respiratory sounds, which limit the capability of respiratory sound analysis. To enhance the effectiveness of the diagnostic tool, several signal denoising methods have been developed. However, the identification of threshold is not done in real-time.

Fattahi et al [26] provide approach for preterm newborns in particular, noise and interference make neonatal lung sound auscultation difficult and frequently unreliable. A lot of the time and frequency of the noise is shared by the heart and lung contents. Additionally, the frequency band of the beneficial components varies from case to case, making it challenging to separate using a set band-pass filter. In this study, a single-channel Blind Source Separation (SCBSS) framework is suggested to distinguish the heart and lung sounds of neonates from the distracting chest sounds captured by a digital stethoscope. The signal is split up into a multi-resolution representation utilising this technique's time-domain decomposition. Although other older age groups, including children and adults, and also the cases with pathological heart and lung sounds, potentially from the same group of subjects, could not be investigated.

Elsetrønning et al [27] examined how different classifiers perform for the given task, decomposition methods like Empirical Mode Decomposition, Ensemble Empirical Mode Decomposition, and Discrete Wavelet Transform are combined with a number of feature extraction techniques like Principal Component Analysis and Autoencoder. The outcomes of employing various decomposition and feature extraction combinations are examined using an open-source dataset retrieved from Kaggle that contains chest auscultation of diverse quality. It has been discovered that the KNN classifier performs best when higher-order statistical and spectral characteristics are supplied into it together with the Mel-frequency cepstral coefficients. However, application of various feature selection methods does not demonstrate the accuracy as well as does not detect anomalies in any time series data.

From the above discussion [22] does not regroup the database in a patient wise manner [23] attains the visual inspection of these IMF does not clearly represent the heart sounds [24] does not suppress the HS contaminations from lung sound signals [25] identification of threshold is not done in manually [26] does not investigated heart and lung sounds potentially from the same group of subjects [27] does not detect anomalies in any time series data.

3. Proposed System

A third heart sound is indicative of accelerated left ventricular dilation and elevated atrioventricular flow. Because this illness is linked to cardiovascular mortality, accurate auscultation of the third heart sound is essential even though it needs experience to detect. Notably, despite the lack of an audible second heart sound, the increased third heart sound was correctly identified**.** The early diastolic fast distension of the left ventricle, which is accompanied by quick ventricular filling and abrupt deceleration of the atrioventricular blood flow, is what primarily causes the third heart sound. The amount of left ventricular inflow deceleration and likelihood of a third heart sound are directly proportional to the transmittal inflow rate and steepness of the rapid filling wave. A third heart sound is most frequently auscultated with mitral regurgitation among valvular disorders. The third heart sound is the first indicator of left heart failure and is linked to cardiovascular mortality, functionally severe heart failure, severe mitral regurgitation, a low ejection fraction, and restrictive diastolic filling. Therefore, it is essential to recognize the third heart sound for quick treatment. The mitral regurgitate murmur often exhibits a steady strength throughout the systole. However, in cases of extensive mitral

regurgitation, there is a rapid rise in the left atrial pressure in late-systole, which is represented in the pronounced v-waves in the recordings of the pressure in the pulmonary artery wedge. The quick increase in left atrial pressure in late systole in this case causes the intensity of mitral regurgitation to lessen in late systole compared to early systole. This is demonstrated by the diminution in the noticeable early systolic regurgitate murmur. Hence proposed method has been developed to detect the third heart sound by using ITD method because the detection is identified without any time delay with several levels of signal decomposition. The third heart sound gallop is a key indicator of ventricular dysfunction. The presence of S3 is a vital clue in predicting the pathological state of heart such as myocardial infraction with chest pain, post myocardial infraction mortality and postoperative pulmonary oedema [28]. The workflow of the proposed method for S3 localization in presence of lung sound is presented in the Fig.1. Initially, the procedure starts with collecting the heart sound and lung sound signals from online resources assorted with biological sounds.

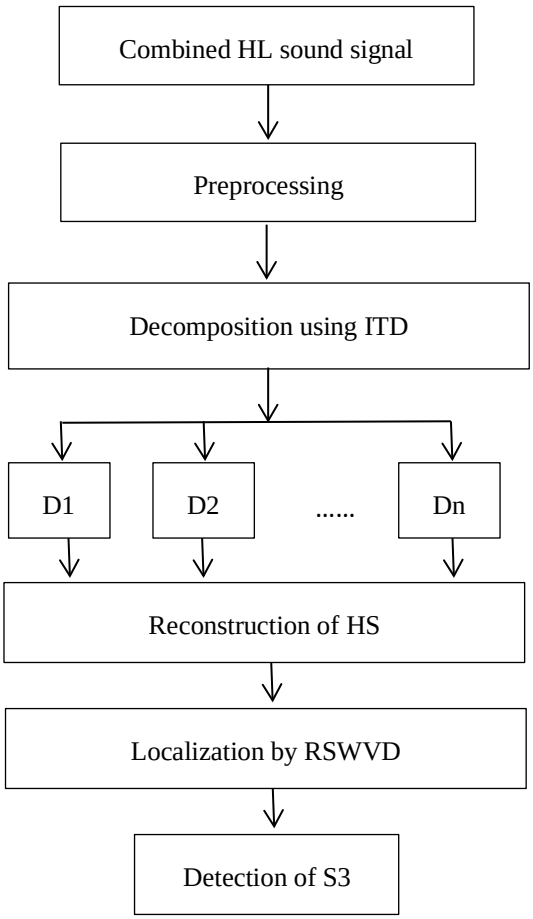

Fig. 1. Proposed workflow

After, these two signals are got together to form a HL sound signal. This combined signal is sampled at 44.1kHz and then normalized in amplitude. This normalized signal is then decomposed in to six components using ITD. The decomposed components undergo analysis where mean frequencies are extracted. The heart sound signal is reconstructed with the components occupying the frequency range of input heart sound. Further, the time frequency energy is examined on the reconstructed heart signal using RSWVD. Finally, the S3 is detected based on the time separation of S2 and S3.

4. Methods

4.1. Intrinsic Time Scale Decomposition

This decomposition is a special class of approach in preserving the structural and phase information. This was introduced by Frei and Osorio [29]. In ITD, for a given input signal the extrema are determined in real time. Now consider the extrema $\{\tau_{k-2}, \tau_{k-1}, \tau_k, \tau_{k+1}\}$, at τ_{k-1} the ITD wants to know the local maximum or the local minimum values at τ_k and τ_{k+1}. After the detection, the baseline signal is constructed in the interval $[\tau_k, \tau_{k+1}]$ by finding the low frequency nodes. The obtained baseline signal between the nodes is observed as the linear transformation of the input signal. Subtracting this low frequency baseline component from the loaded input signal results in high frequency proper rotation component. The mathematical analysis for this approach is described here. To decompose a signal, X_t, into low and high frequency components, two operators are introduced in ITD technique. To extract a low frequency baseline

component(B_t), operator,$\mathcal{L}$, is applied and high frequency proper rotation component (R_t) is extracted by the operator, $\mathcal{H}$.

Then, the X_t is represented as a linear combination of B_t and R_t given as

$$X_t = B_t + R_t \tag{1}$$

Where the $B_t = \mathcal{L}X_t$ provides a low frequency baseline component and $R_t = (1 - \mathcal{L})X_t$ gives a high frequency proper rotation component. Typically, the decomposition is initiated by extracting B_t by a piecewise linear operator, $\mathcal{L}$, which is defined for the interval $(\tau_k, \tau_{k+1}]$ as

$$\mathcal{L}X_t = B_t + (B_{k+1} - B_k)\left(\frac{X_t - X_k}{X_{k+1} - X_k}\right),\ t \in (\tau_k, \tau_{k+1}] \tag{2}$$

Here X_k and B_k represents $X(\tau_k)$ and $B(\tau_k)$ respectively. Where B_{k+1} can be obtained as follows:

$$B_{k+1} = \alpha X_k + (1 - \alpha)X_{k+1} + \alpha\left(\frac{\tau_{k+1} - \tau_k}{\tau_{k+2} - \tau_k}\right)(X_{k+2} - X_k) \tag{3}$$

In the interval$(\tau_k, \tau_{k+1}]$, X_t is monotonic in nature, since it is monotonic the components B_t and R_t are also monotic. The value of gain control parameter α is typically fixed at 0.5 to process the low frequency baseline component. Note, if $\alpha = 0$, the component B_t is same as the X_t and if $\alpha = 1$, the resultant signal consists of only the components with low frequencies. After the extraction of B_t the process is repeated considering the B_t as input until a desired decomposition is obtained.

$$\mathcal{H}X_t = (1 - \mathcal{L})X_t = X_t - B_t \tag{4}$$

Finally, the high frequency proper rotation component (R_t) is obtained from (4). Further, instantaneous amplitude and frequencies for each decomposed component can be calculated for time-frequency analysis.

4.2. Smoothed Pseudo Wigner Ville Distribution

Josefin and Maria [19] suggested that Reassigned smoothed Pseudo Wigner Ville distribution (RSWVD) is the most competent method in localizing closely spaced frequency components. The advantage of reassignment method is that it results in smoothing of the "mother-distribution" [20]. SWVD is effective for PCG signal analysis as it can localize the low energy and closely spaced components present in the heart signal [13]. SWVD is an extended version of Wigner Ville distribution (WVD), provides rich time and frequency resolution. The Wigner Ville distribution is defined as

$$W_{wvd}(t, f) = \int_{-\infty}^{+\infty} v(t + \tau)\, v^*(t - \tfrac{\tau}{2})\, e^{-j2\pi f\tau}\, d\tau \tag{5}$$

The above equation produces spurious harmonics due to its quadratic distribution character. These harmonics are known as cross terms results from (5). Consider, the equation consists of two harmonics say $v(t) = v_1(t) + v_2(t)$, then the real part of $W_{wvd}(t, f)$ consists of$v_1(t).v_1(t) + v_2(t).v_2(t) + 2v_1(t).v_2(t)$. The third term $2v_1(t).v_2(t)$ is referred to as a cross term which is an undesirable one. The cross terms hinder the performance in analyzing the low frequency aspects of the signal. Partially, this problem can be suppressed by using smoothed pseudo-Wigner Ville distribution. SWVD is the extended genre of WVD which uses a window, able to suppress the cross terms given in (6).

$$\text{WSPWD } t,f = u1t * Wwvdt,f * U2(f) \tag{6}$$

Where $u_1(t)$ and $U_2(f)$ are the window functions for smoothing. The above smoothing function results in uneven distribution of energy around the centre point, which doesn't represent the actual region. So the reassignment is suggested as it relocates the time-frequency of the higher energy regions and gets the precise location information. In this connection, at a point say (t, f) should be relocating to another point (t', f') by the reassignment. This is given by following expressions [16]

$$Re_{SPWD}(t, f) = \iint_{-\infty}^{+\infty} W_{wvd}(t, f)\ \delta(t - t_{sp}(t', f'))\ \delta(f - f_{sp}((t', f'))\, dt'\, df' \tag{7}$$

Where

$$t_{sp} = \frac{W_{SPWD}(t, f)\ .\ t - \left(t\,.\,u_1(t)\right) * W_{wvd}(t, f) * U_2(f)}{W_{SPWD}(t, f)}$$

$$f_{sp} = \frac{W_{SPWD}(t,f)\ .\ t - u_1(t) * W_{wvd}(t,f) * (f.U_2(f))}{W_{SPWD}(t,f)} \quad (8)$$

In (7), δ is the function which relocates the centre point to the specified values by $t_{sp}(t', f')$ and $f_{sp}(t', f')$. This gives accurate localization of the closely spaced signal components.

5. Experiment

In this work LS signals are taken from Littman database [21] and HS signals are collected from both Littman database and Washington database [22]. Total of 36 combinations of HL sound signals are generated for this work. These 36 combinations of consists of 144 cardiac cycles containing S3 are processed in MATLAB R2018a. The combined signal is sampled at 44.1 kHz is loaded in to the proposed method. This signal is then normalized in amplitude and then given for decomposition using ITD. The ITD operation divides the signal into low frequency baseline and high frequency proper rotation components for all the iterations.

The fig. 2 illustrates the decomposed baseline components (D1, D2…D9) of a HS signal. A raw heart signal with normalized amplitude is allowed here for the decomposition to observe the number of iterations required to get the last components with almost zero frequency using EMD, HVD and ITD. The monotonic trend is observed in the ninth decomposed component for ITD of this signal and tenth component for EMD as well as for HVD. As the number of iterations is less in the case of ITD, the better will be the computational time compared with EMD and HVD. In this work, the first six decomposed components are considered. As the seventh and above components shows much deviation from the mean frequency of the heart signal, they are not considered for further processing.

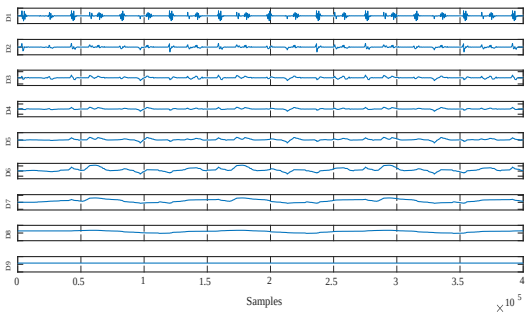

Fig. 2. Decomposed baseline components using ITD

However, a monotonic trend is observed in the ninth decomposed component. After the decomposition, the reconstruction of the heart signal was made by the combination of last four decomposed components out of six. In addition to that, the reconstruction of the lung signal was made by the combination of first two decomposed components. The reason for selecting the components for reconstruction is based on mean frequency (MNF) analysis. Later, RSWVD is applied on the reconstructed signal for the exact location information. Lastly, based on the timing information S3 is detected and the detection accuracy is calculated.

6. Results and Discussions

This section includes a thorough analysis of the performance of the proposed system, the implementation results simulated in the MATLAB platform, and a comparison section to make sure the suggested system is appropriate for detection of heart and lung sound [30-33]. The system specification is given below,

Platform	**:** MATLAB R2018a
OS	**:** Windows 10
Processor	**:** 64-bit Intel processor
RAM	**:** 8 GB RAM

6.1 Dataset Description

LS signals are taken from Littman database and HS signals are collected from both Littman database and Washington database. Total of 36 combinations of HL sound signals are generated for this work. These 36 combinations of consists of 144 cardiac cycles containing S3. The combined signal is sampled at 44.1 kHz is loaded.

6.2 Stimulation output of proposed model

The heart and lung sound signals are collected separately from the both the public databases mentioned in the previous section. The corresponding heart and lung signals are represented in fig. 3. The combined HL sound signal

consists of normal and abnormal conditions of both heart and lung. The input to the proposed work is this combined HL sound signal. A total of 36 combinations are examined in the process of S3 detection. At first, the mixed HL sound signal is sampled at 44100Hz and then the amplitude is normalized between -1 to +1. Next, it is decimated by a factor 20 to reduce the number of samples. This completes the preprocessing stage.

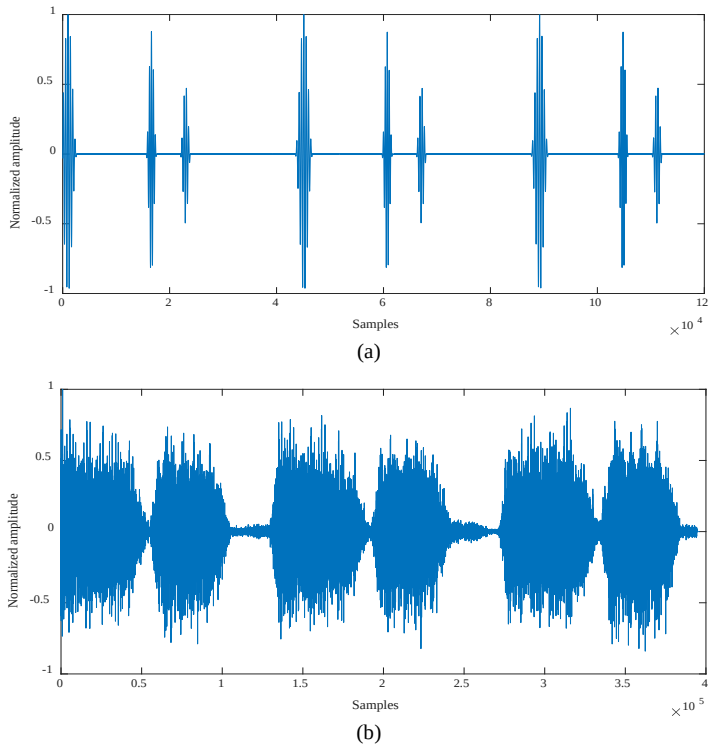

Fig. 3. Heart and Lung sound signal for preprocessing

The preprocessed signal is shown in fig (4) is allowed to decompose using ITD. Detection of third heart sound in recognizing the heart failures is usually masked by additional sounds during PCG signal acquisition with the help of ITD. The ITD decomposes the combined HL sound signal into low frequency baseline and high frequency proper rotation components.

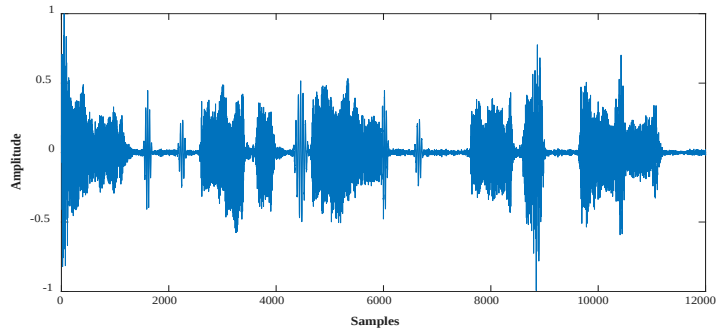

Fig. 4. Combined HL sound signal

In this work, the first six decomposed low frequency components from D1 to D6 are considered based on mean frequencies analysis. The MNF for a given power spectrum [23] is given by

$$\mathrm{MNF} = \frac{\sum_{j=1}^{M} f_j P_j}{\sum_{j=1}^{M} P_j} \tag{9}$$

Where f_j, is the frequency at bin j of the spectrum and P_j is the power spectrum value at j^{th} bin and L is the length of the frequency bin. The Mean (μ) and standard deviation (σ) obtained for MNFs of the decomposed components for 36 combined signals are presented in the Table 1.

Table 1.Values of the parameters μ and σ in Hz of the MNFs for the first six decomposed components

Decomposed component	MNF		Decomposed component	MNF	
	μ	σ		μ	σ
D1	655	57	D4	33	9
D2	355	56	D5	15	4
D3	95	25	D6	4	3

The first six decomposed components are shown in fig. 5. However, a monotonic trend is observed in the ninth decomposed component. The components D7, D8 and D9 are not considered for reconstruction, as their MNFs are much deviated from the mean frequency of the actual heart signal which is at 112Hz.

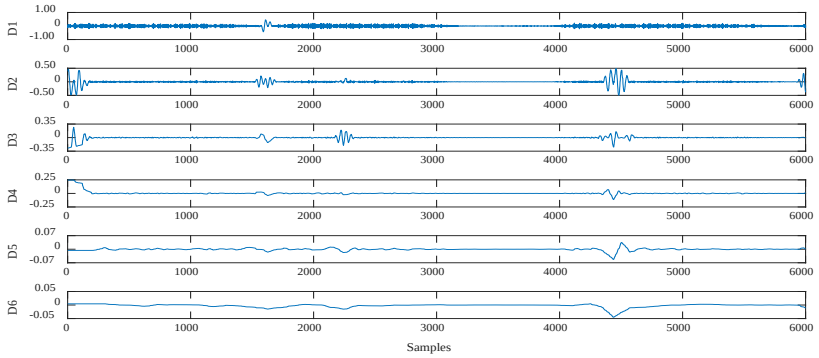

Fig. 5. First six decomposed components from D1 to D6

Observing the mean frequencies of the components from D1 to D6, for the reconstruction of lung sound signal, D1 and D2 are considered and D3, D4, D5 and D6 are for the reconstruction of heart sound signal. The reconstructed HS signal from the defined components is shown in the fig (6).

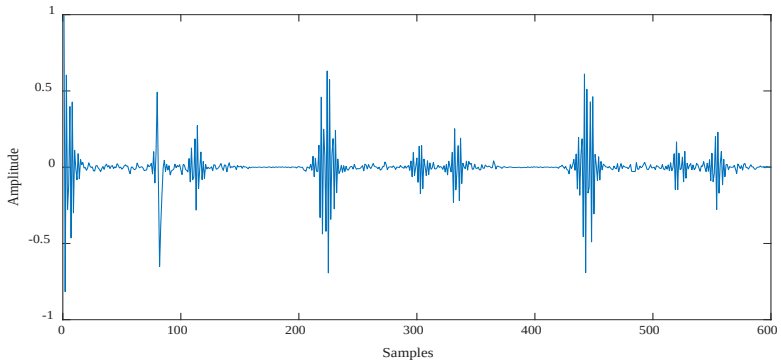

Fig. 6. Reconstructed HS signal

The restoration of the heart signal is very important as this signal will undergo localization for detecting S3. Hence quantitative parameters are chosen for error analysis between actual and reconstructed signals. The parameters used in this work are mean square error (MSE), signal to error ratio (SER) and correlation coefficient (ρ). These are expressed as:

$$\mathrm{MSE} = \frac{1}{\mathrm{N}}\sum_{\mathrm{n}=1}^{\mathrm{N}}(\mathrm{X_{as}[n]} - \mathrm{X_{rs}[n]})^2 \tag{10}$$

$$\mathrm{SER(dB)} = 10 \times \log_{10}\frac{\sum_{\mathrm{n}=1}^{\mathrm{N}}(\mathrm{X_{as}[n]})^2}{\sum_{\mathrm{n}=1}^{\mathrm{N}}(\mathrm{X_{as}[n]}-\mathrm{X_{rs}[n]})^2} \tag{11}$$

$$\rho = \frac{\sum_{\mathrm{n}=1}^{\mathrm{L}} \mathrm{X_{as}[n]}\,\mathrm{X_{rs}[n]}}{\sqrt{\sum_{\mathrm{n}=1}^{\mathrm{L}} \mathrm{X_{as}}^2\mathrm{[n]}\quad \mathrm{X_{rs}}^2\mathrm{[n]}}} \tag{12}$$

$\mathrm{X_{as}[n]}$ is the actual HS signal and $\mathrm{X_{rs}[n]}$ is the reconstructed HS signal after the decomposition. Similarly, the quantitative analysis is made using EMD and HVD.

Table 2. Performance comparison between EMD, HVD and ITD

Method	MSE		SER(dB)		ρ	
	μ	σ	μ	σ	μ	σ
EMD	0.0061	0.005	6.010	4.760	0.8777	0.09
HVD	0.0064	0.004	6.050	5.080	0.9124	0.09
ITD	0.0059	0.007	7.180	6.720	0.9377	0.11

The obtained values of MSE, SER and ρ in the Table 2 illustrates that the superiority of ITD over EMD and HVD. This infers the productivity of the proposed method is competent in separating heart sounds from lung sounds. Furthermore, by comparing the proposed work with power spectral density, the performance of the work is increased Fig. 7 shows the estimated and plotted PSDs for the actual heart sound signal and the reconstructed heart sound signal following the separation from the lung sound. The PSD estimates how well the separation from lung sound works. If the PSD of the real heart sound signal matches the PSD of the reconstructed heart sound signal, the estimation was accurate.

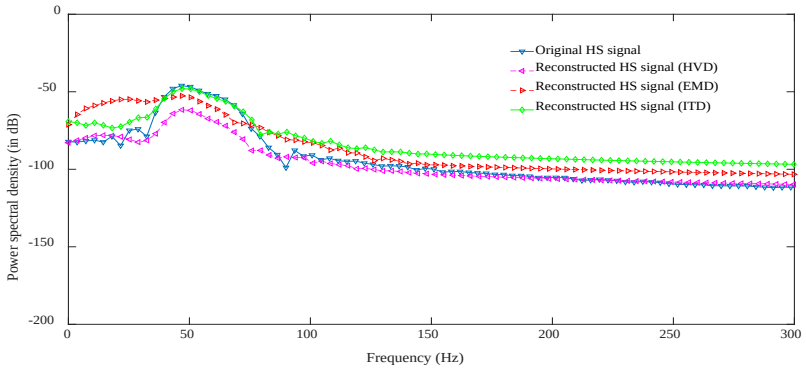

Fig. 7. PSD plot of original HS signal and reconstructed HS signals of EMD, HVD & ITD methods

The PSD plot of the reconstructed signal must coincide with the PSD plot of the original signal in order for the reconstruction of the HS signal using LS signal cancellation to be effective. Fig. 7 displays the PSD plot of the original HS signal as well as the reconstructed signals produced by the EMD, HVD, and ITD approaches. As seen in the figure, PSD of the reconstructed signal using ITD is more similar to the original HS signal than EMD and HVD.

RSWVD's visual analysis of TFR plots reveals S3 to be present. The entire signal is split up into little cardiac segments to find S3. S1, S2, and S3 are the 400ms-long components that make up each segment. Following deconstruction, cardiac cycles are examined visually and a random selection is made for further processing. The segmentation of each of the chosen cardiac cycles follows the pattern in fig. 8. A whole systolic phase is followed by a portion of the diastolic period in the pattern. The following S3 is found in the 400ms overall clip: (A) Verify the three components' real placements in relation to their energy levels first. (a) After that, confirm S3 by calculating the time difference between S2 and S3 [13].

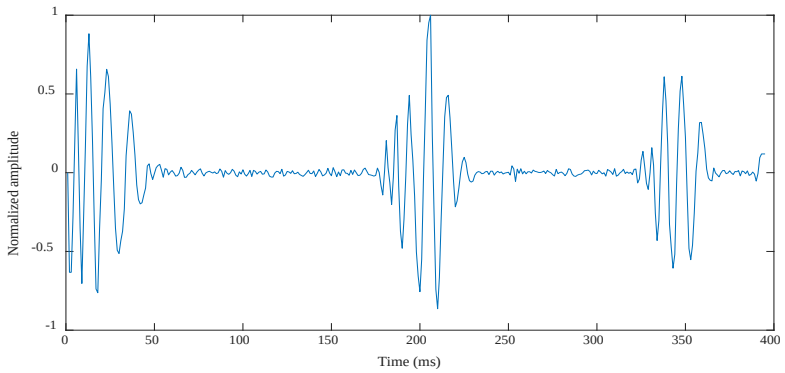

Fig. 8. Segment from a cardiac cycle.

A particular segment is considered from the reconstructed heart signal to delineate the localization process in the detection of S3. A fixed pattern is assigned as shown in fig. 8 is given for 400ms of total cardiac cycle. Total of 44 segments are allowed for time frequency analysis. With the help of normalization, medium pitched Broncho vesicular sounds over the mainstream bronchi, between the scapulae, and below the clavicles. Soft, breezy, low-pitched vesicular breath sounds over most of the peripheral lung fields can be detected by using reassignment method in which the time

frequency energy is examined. The time frequency representation by SWVD of that segment is displayed in fig .9. From the fig .9, S3 is not perfectly outlined comparatively with S1 and S2. Further, the TFR plots are reassigned and the outcome is depicted in fig .10. The positions of the three heart sounds can be estimated but this does not give the actual positional information. The RSWVD is constructed to illustrate further to get the corresponding positional timing to confirm S3 presence. To know the exact positions of S1, S2 and S3, the normalized reassigned plot is to be consider**,** in which the vertical axis act for normalized frequency and horizontal refer to time. This completes the estimation of actual positions of the components.

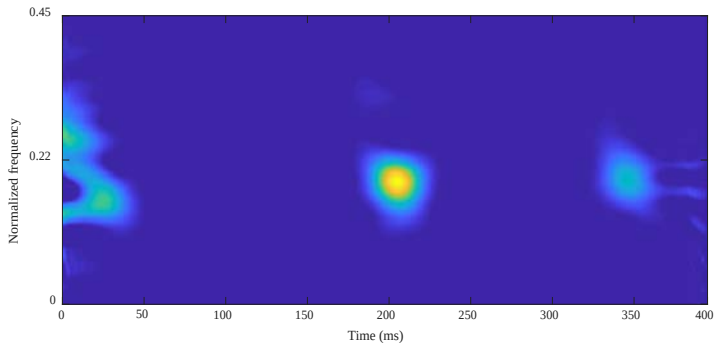

Fig. 9.SWVD - TFR plot of extracted cardiac segment

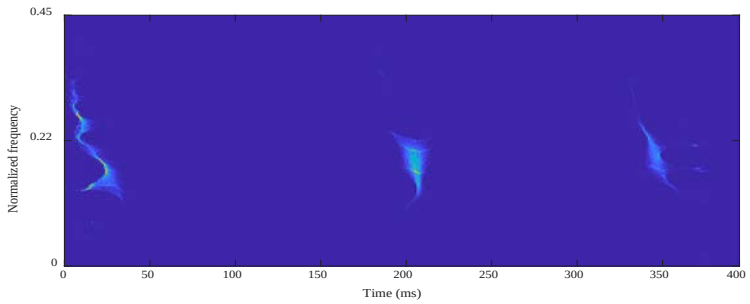

Fig. 10. RSWVD - TFR plot of extracted cardiac segment.

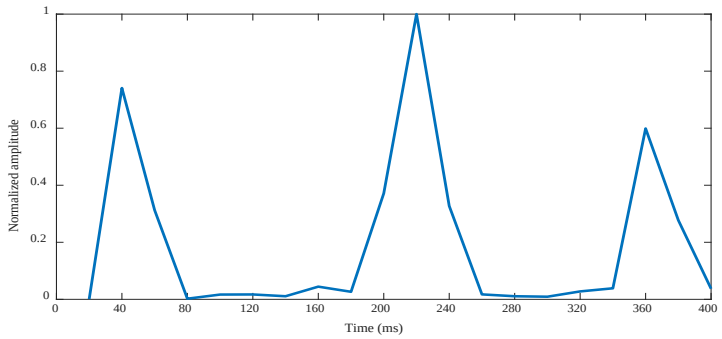

Fig. 11. Normalized amplitudes plot with time indicated on the x-axis

Calculate the time difference between S2 and S3 at this point to verify S3. The time difference between S2 and S3 has a mean and standard deviation of 122 and 10.2 ms, as can be seen from 44 segments of time frequency analysis. In fig. 11, the presence of S3 is further supported by the lowest peak, which denotes the position of S3 in reality. The S3 detection process is now complete, and the proposed work's performance is evaluated by comparing its parameter accuracy to that of competing approaches.

$$\text{Accuracy} = \frac{\text{Total number of detected S3s}}{\text{Total number of detected S1s or S2s}} \times 100\% \quad (13)$$

By applying smoothed pseudo-Wigner Ville distribution (SWVD) with reassignment, the location of S3 is detected. The proposed method is performed on 36 combinations consists of 144 cardiac cycles containing S3 obtained from different online databases. The parameter accuracy from (12) is considered from [13] is calculated and compared with

EMD [10] and HVD [13]. The obtained values are listed in the Table 3. The EMD and HVD are not always functional in all the cases where S3 is weak.

Table 3. Accuracy results of EMD, HVD and ITD

Components	Methods		
	EMD	HVD	ITD
S1	44	44	44
S2	44	44	44
S3	36	38	42
Accuracy (%)	81.8	86.3	95.4

The spectral overlap of these heart and lung sounds allows a challenging task in separation. The localization is a crucial step in detecting the weak sounds. The accuracy of the proposed work is obtained as 95.4% marking that this study is more suitable for detection of S3 than EMD and HVD.

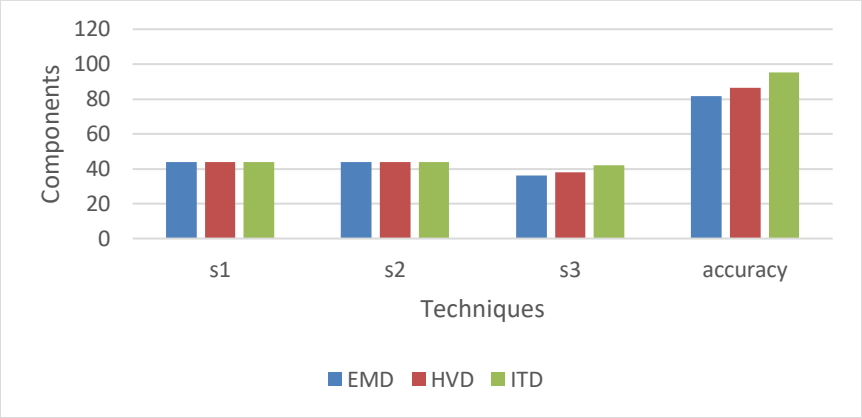

Fig. 12. Comparison of proposed with existing techniques

Fig. 12 depicts the comparison of accuracy. The proposed system is compared with existing techniques such as EMD and, HVD. The accuracy of proposed system has the maximum value of 95.4 whereas the accuracy EMD and HVD are 81.8, and 86.3. The utility of heart and lung sound for detecting mechanical abnormalities of the respiratory system in mechanically ventilated patients is the immediate postoperative period after cardiac surgery. This showed that neither the presence nor the absence of abnormal respiratory sounds was associated with mechanical abnormalities of the respiratory system, and that accuracy detection is failed to identify patients with abnormal respiratory mechanics. Hence ITB was proposed to identify the correct accuracy of heart and lung sounds by decomposition process. The accuracy of proposed model is high whereas the accuracy of EMD is low

7. Conclusion

Detecting the Third Heart Sound by Separation and Localization from Lung Sound using Intrinsic Time Scale Decomposition method has been proposed in this research, the first heart sound (S1) and the second heart sound (S2), produced by the closing of the atrioventricular valves and the closing of the semilunar valves cause some suppressing due to the inflammation of atrioventricular and semilunar valves. Hence the issue is tackled by ITD method that detect the heart sound(S3) without any time delay. The decomposed components by ITD method provide relevant information for the formation of HS signal. The mean frequency study is found to ignore some of the decomposed components which are not useful for HS signal reconstruction. Subsequently, the reconstructed signal from careful perusal of mean frequencies is then localized using RSWVD. Finally, the S3 is located by measuring the time difference value between S2 and S3. When compared to existing techniques the proposed method has a high accuracy value of 95.4% is achieved. As a result, the proposed approach eliminates the shortcomings of the existing methodologies.

References

[1] Nabih-Ali, M., El-Dahshan, E.S.A. and Yahia, A.S., 2017. A review of intelligent systems for heart sound signal analysis. *Journal of medical engineering & technology*, *41*(7), pp.553-563.

[2] Chen, J., Sun, S., Zhang, L.B., Yang, B. and Wang, W., 2021. Compressed sensing framework for heart sound acquisition in internet of medical things. *IEEE Transactions on Industrial Informatics*, *18*(3), pp.2000-2009.

[3] Queyam, Abdullah Bin, Sharvan Kumar Pahuja, and Dilbag Singh, "Doppler ultrasound based non-invasive heart rate telemonitoring system for wellbeing assessment," *International Journal of Intelligent Systems and Applications,* vol. 11, no. 12, pp. 69, 2018.

[4] Nayak, S., Gourisaria, M.K., Pandey, M. and Rautaray, S.S., 2019. Heart Disease Prediction Using Frequent Item Set Mining and Classification Technique. *International Journal of Information Engineering & Electronic Business*, *11*(6).
[5] M. El-Segaier, O. Lilja, S. Lukkarinen, L. Sörnmo, R. Sepponen, and E. Pesonen, "Computer-Based Detection and Analysis of Heart Sound and Murmur," *Annals of Biomedical Engineering*, pp. 937–942, 2005.
[6] Nersi, Ruban, G. P. S. Arneja, K. Bansal, and Noel Mathew, "Heart sound analysis using lab View," *Journal of Theoretical & Applied Information Technology*, pp. 1029-1033, 2012.
[7] R. Nersisson, and M. M. Noel, "Heart sound and lung sound separation algorithms: a review." *Journal of Medical Engineering & Technology*, pp. 13–21, 2016.
[8] A. L. Padilla-Ortiz, and D. Ibarra, "Lung and Heart Sounds Analysis: State-of-the-Art and Future Trends," *Critical Reviews in Biomedical Engineering*, pp. 33–52, 2018
[9] V. K. Iyer, P. A. Ramamoorthy, H. Fan, and Y. Ploysongsang, "Reduction of heart sounds from lung sounds by adaptive filtering," *IEEE Trans. Biomed*, pp. 1141–1148, 1986.
[10] J. Gnitecki, Z. Moussavi, and H. Pasterkamp, "Recursive least square adaptive noise cancellation filtering for heart sound in lung sounds recording," *Proceedings of the 25th Annual International Conference of the IEEE Engineering in Medicine and Biology Society Mexico*, pp. 2416–2419, 2004.
[11] I. Hossain, and Z. Moussavi, "An overview of heart-noise reduction of lung sound using wavelet transform based filter," *Proceedings of the 25th Annual International Conference of the IEEE Engineering in Medicine and Biology Society*, pp. 458–461, 2003
[12] M. T. Pourazad, Z. Moussavi, and G. Thomas, "Heart sound cancellation from lung sound recordings using time-frequency filtering," *Medical & Biological Engineering & Computing*, vol. 44, no. 3, pp. 216–225, 2006.
[13] A. Yadollahi, and Z. M. K. Moussavi, "A Robust Method for Heart Sounds Localization Using Lung Sounds Entropy," *IEEE Transactions on Biomedical Engineering*, pp. 497–502,2006.
[14] A. Mondal Bhattacharya, and G. Saha, "Reduction of heart sound interference from lung sound signals using empirical mode decomposition technique," *Journal of Medical Engineering & Technology*, pp. 344–353, 2011.
[15] Malihe Molaie, and Mohammad Hassan Moradi, "Heart Sound Localization in Respiratory Sounds Based on Singular Spectrum Analysis and Frequency Features," pp. 824-832, 2015.
[16] B. Sai Bharadwaj, and Ch. Sumanth Kumar, "Classification of the Third and Fourth Heart Sounds using Intrinsic Time-Scale Decomposition and Support Vector Machine Technique," *International Journal of Innovative Technology and Exploring Engineering*, pp. 1172-1177, 2019.
[17] S. Barma, B. W. Chen, W. Ji, S. Rho, C. H. Chou, and J. F. Wang, "Detection of the Third Heart Sound Based on Nonlinear Signal Decomposition and Time–Frequency Localization," *IEEE Transactions on Biomedical Engineering*, pp. 1718–1727, 2016.
[18] E. Sejdic, and J. Jiang, "Comparative study of three time-frequency representations with applications to a novel correlation method," IEEE *International Conference on Acoustics, Speech, and Signal Processing, Canada*, pp. 633-634, 2004.
[19] D. Kumar, P. Carvalho, M. Antunes, J. Henriques, A. S. Melo, R. Schmidt, and J. Habetha, "Third Heart Sound Detection Using Wavelet Transform-Simplicity Filter," *29th Annual International Conference of the IEEE Engineering in Medicine and Biology Society*, *France*, pp. 1277-1281, 2007.
[20] J. M. Stark Ammar, and Hansson-Sandsten, "Evaluation of Seven Time-Frequency Representation Algorithms Applied to Broadband Echolocation Signals," *Advances in Acoustics and Vibration*, pp. 1–13, 2015.
[21] Johnston, and S. P. Collins, "Storrow AB The third heart sound for diagnosis of acute heart failure. Current Heart Failure Reports," pp. 164–169, 2007.
[22] Zeng, Wei, et al. "A new approach for the detection of abnormal heart sound signals using TQWT, VMD and neural networks," *Artificial Intelligence Review*, vol. 54, no. 3, pp. 1613-1647, 2021.
[23] Altuve, Miguel, Luis Suárez, and Jeyson Ardila, "Fundamental heart sounds analysis using improved complete ensemble EMD with adaptive noise," *Biocybernetics and Biomedical Engineering*, vol. 40, no. 1, pp. 426-439, 2020.
[24] Haider, and Nishi Shahnaj, "Respiratory sound denoising using empirical mode decomposition, hurst analysis and spectral subtraction," *Biomedical Signal Processing and Control*, vol. 64, pp. 102313, 2021.
[25] B. Sangeetha, and R. Periyasamy, "Performance Metrics Analysis of Adaptive threshold Empirical Mode Decomposition Denoising method for suppression of noise in Lung sounds," *2021 Seventh International conference on Bio Signals, Images, and Instrumentation (ICBSII). IEEE*, 2021.
[26] Fattahi, Davood, et al. "A Blind Filtering Framework for Noisy Neonatal Chest Sounds," *IEEE Access*, vol. 10, pp. 50715-50727, 2022.
[27] Elsetrønning, Andrine, et al. "On the effectiveness of signal decomposition, feature extraction and selection on lung sound classification". *arXiv preprint arXiv:2012.11759* (2020).
[28] S. Raman, and B. N. Weber, "Detecting the gallop: the third heart sound and its significance," *The Medical Journal of Australia*, pp. 198–199, 2017.
[29] M. G. Frei, and I. Osorio, "Intrinsic time scale decomposition: time-frequency-energy and real time filtering of non-stationary signals," *Proceedings of the Royal Society A: Mathematical. Physical and Engineering Sciences*, pp. 321-342, 2006.
[30] François Auger, Patrick Flandrin, Yu-Ting Lin, Stephen Mclaughlin, Sylvain Meignen, et al., "Time Frequency Reassignment and Synchro squeezing: An overview," *IEEE Signal Processing Magazine. Institute of Electrical and Electronics Engineers*, pp. 32-41, 2013.
[31] Heart and Lung Sounds Library. Available: http://solutions.3mae.ae/wps/portal/3M/en_AE/3M-Littmann-EMEA/stethoscope/littmann-learning-institute/heart-lungsounds/heart-lung-sound-library/.
[32] Heart Sounds & Murmurs, Accessed, Oct. [Online]. Available: https://depts.washington.edu/physdx/heart/demo.html
[33] A. Phinyomark, S. Thongpanja, H. Hu, P. Phukpattaranont, and C. Limsakul, "The Usefulness of Mean and Median Frequencies in Electromyography Analysis," *Computational Intelligence in Electromyography Analysis - A Perspective on Current Applications and Future Challenges*, 2012.

Authors' Profiles

Sai Bharadwaj B is currently pursuing his Ph.D. degree in department of Electrical, Electronics and Communication Engineering, GITAM Institute of Technology, GITAM Deemed to be University, Rishikonda, Visakhapatnam, Andhrapradesh, India. His research interests include bio medical signal processing, speech processing, machine learning.

Ch.Sumanth Kumar received the Ph.D degree from the department of Electrical, Electronics and Communication Engineering, GITAM Institute of Technology, GITAM Deemed to be University, Rishikonda, Visakhapatnam, Andhrapradesh, India. He is currently working as an Professor in GITU, Visakhapatnam, India. His research interests include bio medical signal processing and automatic control.

How to cite this paper: Sai Bharadwaj B, Ch. Sumanth Kumar, "Detecting the Third Heart Sound: Separation and Localization from Lung Sound using Intrinsic Time Scale Decomposition", International Journal of Image, Graphics and Signal Processing(IJIGSP), Vol.15, No.1, pp. 23-35, 2023. DOI:10.5815/ijigsp.2023.01.03